ACS APPLIED MATERIALS & INTERFACES

Research Article

www.acsami.org

Poly(L-lysine)-*graft*-folic acid-coupled poly(2-methyl-2-oxazoline) (PLL-*g*-PMOXA-*c*-FA): A Bioactive Copolymer for Specific Targeting to Folate Receptor-Positive Cancer Cells

Yin Chen,[†,#] Wenbin Cao,[‡,#] Junli Zhou,[§] Bidhari Pidhatika,[∥] Bin Xiong,[⊥] Lu Huang,[⊥] Qian Tian,[⊥] Yiwei Shu,[⊥] Weijia Wen,[‡] I-Ming Hsing,[†,§] and Hongkai Wu*[,†,⊥]

[†]Division of Biomedical Engineering, The Hong Kong University of Science and Technology, Hong Kong, China

[‡]Department of Physics, The Hong Kong University of Science and Technology, Hong Kong, China

[§]Department of Chemical and Biomolecular Engineering, The Hong Kong University of Science and Technology, Hong Kong, China

[∥]Department of Industrial Chemical Engineering, College of Industrial Management, Ministry of Industry, Jl. Letjen Suprapto No. 26 Cempaka Putih Jakarta 10510, Indonesia

[⊥]Department of Chemistry, The Hong Kong University of Science and Technology, Hong Kong, China

Supporting Information

ABSTRACT: In this study, we present the preparation, characterization and application of a novel bioactive copolymer poly(L-lysine)-*graft*-folic acid-coupled poly(2-methyl-2-oxazoline) (PLL-*g*-PMOXA-*c*-FA), which has a specific interaction with folate receptor (FR)-positive cancer cells. Glass surface immobilized with PLL-*g*-PMOXA-*c*-FA was demonstrated to be adhesive to FR-positive cancer cells (HeLa, JEG-3) while nonadhesive to FR-negative ones (MCF-7, HepG2) in 3 h. The specific interaction between conjugated FA on the substrate and FRs on the cells could hardly be inhibited unless a high concentration (5 mM) of free FA was used due to the multivalent nature of it. The FA functionality ratio of the copolymer on the substrate had a significant influence on the adhesion of HeLa cells, and our experiments revealed that the affinity of the substrate to the cells declined dramatically with the decrease of functionality ratio. This was believed to be caused by the polydispersity of PMOXA tethers, as supported by GPC and ToF-SIMS data. As a proof of concept in the application of our material, we demonstrated successful recovery of HeLa cells from mixture with MCF-7 (1:100) on the copolymer-coated glass, and our results showed that both high sensitivity (95.6 ± 13.3%) and specificity (24.3 ± 8.6%) were achieved.

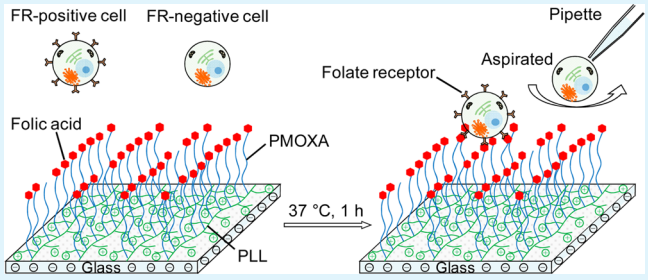

KEYWORDS: *poly(2-methyl-2-oxazoline), folic acid, bioactive copolymer, specific targeting, cancer cells*

1. INTRODUCTION

Bioactive surfaces are the surfaces functionalized with biomolecules for specific interactions with biological objects.[1] These bioactive molecules include enzyme, antibody, nucleic acid, antibiotic, and peptide. Their targets are miscellaneous, including small biomolecules, proteins, DNA molecules, microbes, and even mammalian cells.[2−9] Such surfaces are of great importance in various biomedical applications, such as tissue engineering, biosensors, artificial implants, and drug delivery systems.[2,3,10−12] For instance, the surfaces immobilized with nuclease for anti-infection and tissue integration, antibody for immunoassay, antibiotics for antibiosis and anticoagulant (e.g., heparin) for preventing thrombosis.[3,4,7,13,14] To obtain a superior performance, the bioactive surfaces need to be meticulously designed so that there are sufficient numbers of bioactive molecules on top that can readily interact with their targets.[1] In the meantime, the surfaces must be able to inhibit nonspecific interactions with other molecules.[1] To achieve this goal, antifouling polymers have been extensively employed, among which poly(ethylene glycol) (PEG) as the "gold standard" is most frequently used due to its bioinertness and biocompatibility.[15,16] However, as a hydrolytically degradable polymer, there is a limitation for PEG under harsh environments or in the long term application.[17−20] In addition, PEG or PEGylated products can undergo thermo-decomposition in air at high temperature during the fabrication process.[21,22] As a result, alternative polymers such as polysaccharides, peptidomimetic, and zwitterionic polymers have been developed.[23−30]

Poly(2-methyl-2-oxazoline) (PMOXA), which is a peptide-like polymer, has attracted much attention in recent years.[19,31−37] PMOXA is similar to PEG structurally in the aspect that each oxygen atom in the backbone is replaced by a nitrogen atom linked to an acetyl group.[31] Previous studies have demonstrated that PMOXA has a comparable antifouling

Received: November 29, 2014
Accepted: January 12, 2015
Published: January 12, 2015

DOI: 10.1021/am508399w
ACS Appl. Mater. Interfaces 2015, 7, 2919−2930

property and a better stability than PEG in a range of different aqueous solutions and under cell culture conditions.[19,20,31,32] In addition, the synthesis of PMOXA is more convenient than that of PEG because the initial monomer of PMOXA is liquid up to 110 °C under ambient pressure compared to the gaseous monomer of PEG at room temperature, thus allowing a safer and better controlled polymerization.[38,39] Although functional end groups can be readily introduced by initiators and terminating agents, few studies reported the application of PMOXA in creating bioactive surfaces.[40−43]

Here, we describe the preparation of a novel bioactive copolymer based on PMOXA, poly(L-lysine)-*graft*-folic acid-coupled poly(2-methyl-2-oxazoline) (PLL-*g*-PMOXA-*c*-FA). Folic acid (FA) is frequently used for targeted drug delivery to cancer cells because folate receptor (FR) is highly expressed in many kinds of malignant cancers compared to normal tissues.[44,45] PLL has been extensively explored for gene and drug delivery due to its capability of easy conjugation with drugs via chemical reaction with the free amine groups on it and the ability to enhance cell penetration due to its polycationic nature.[46−49] It also has applications in the preparation of PEG-based brush-like graft copolymer for the creation of both bioinert and bioactive surfaces via the "grating onto" strategy on negatively charged substrates.[2,3,50,51] It is believed that the copolymer prepared by grafting folic acid-coupled antifouling PMOXA side chains on PLL backbone has the capability to specifically target to FR-positive cancer cells and can be used in cancer-related applications.

2. EXPERIMENTAL SECTION

2.1. Preparation of PLL-*g*-PMOXA-*c*-FA. *2.1.1. Materials.* Ethyl 3-bromopropionate (initiator) and 2-methyl-2-oxazoline (MOXA, monomer) were purchased from Aladdin Reagent (Shanghai, China). Ethylenediamine (terminating agent for polymerization), anhydrous acetonitrile (solvent for polymerization) and dimethyl sulfoxide (DMSO, solvent for folic acid coupling) were provided by Sigma-Aldrich (St. Louis, USA), Fisher Scientific (Loughborough, UK) and Acros Organics (New Jersey, USA), respectively. Coupling agents *N*-(3-(dimethylamino)propyl)-*N*′-ethylcarbodiimide hydrochloride (EDC-HCl) and *N*-hydroxysulfosuccinimide sodium salt (Sulfo-NHS) were bought from Highfine Biotech (Suzhou, China). Folic acid (FA) and poly(L-lysine) hydrobromide (PLL-HBr; M_w, ~21 kDa; PDI, 1.04) were obtained from Sinopharm Chemical Reagent (Beijing, China) and Alamada Polymers (Huntsville, AL), respectively. MOXA was freshly dried by refluxing over KOH under reduced pressure before use. Ethylenediamine was distilled through a Vigreux column in nitrogen gas at 1 atm. Acetonitrile (solvent for polymerization) was purified by Pure-Solv Solvent Purification Systems (Innovative Technology, Shenzhen, China). Unless otherwise stated, all other chemicals were used without further purification.

2.1.2. Polymerization of MOXA. Polymerization of MOXA was initiated with an initiator to monomer ratio of 1:50 or 1:25 so as to obtain two types of PMOXA with distinct lengths and ending groups. Briefly, MOXA (10.2 mL, 120 mmol) was dissolved in acetonitrile (40 mL). Ethyl 3-bromopropionate (310 or 620 μL, 2.4 or 4.8 mmol) was added and polymerization was carried out at 70 °C (15 or 8 h). Subsequently, the reaction was quenched by adding ice pellets into the water bath. The solvent was removed at 40 °C under reduced pressure and white solids were harvested. After that, the shorter PMOXA was hydrolyzed in NaOH solution (1 mol/L, 50 mL) at room temperature for 24 h. The longer PMOXA was terminated with ethylenediamine (8 mL, 120 mmol) before hydrolysis in NaOH solution (1 mol/L, 50 mL) for the same time. Then the pHs of polymer solutions were adjusted to 6−8 with concentrated HCl (37%) prior to purification by dialysis (1000 MWCO tubing, Spectra/Por 7, Spectrum Laboratories, Inc.) against ultrapure water (NANOpure, Thermo Scientific Barnstead, 1 L × 8) for 48 h. Polymers were harvested as white solids with yields of ~50% after lyophilization. The molecular weights and chemical structures of these two types of PMOXAs were determined by gel permeation chromatography (GPC) and proton nuclear magnetic resonance (^{1}H NMR) spectroscopy, respectively.

2.1.3. Synthesis of PMOXA-c-FA. FA (441 mg, 1.00 mmol) and EDC-HCl (1.917 g, 10.00 mmol) were dissolved in DMSO (15 mL), which was subjected to agitation in the dark at ambient temperature for 4 h to activate the carboxyl groups of FA. Subsequently, PMOXA-NH_2 (1.2 g, ~0.27 mmol) was added, and the agitation was continued for 20 h. After that, 15 mL of phosphate buffer (PB, 0.01 M, pH = 7.4) was added in the solution, and the mixture was dialyzed (1000 MWCO tubing, Spectra/Por 7, Spectrum Laboratories Inc.) against PB (2 L × 12) for 3 days and ultrapure water (2 L × 6) for 2 days. Polymer was harvested as orange powder with a yield of ~80% after lyophilization. The molecular weight and chemical structure of PMOXA-*c*-FA were determined by GPC and ^{1}H NMR spectroscopy, respectively.

2.1.4. Preparation of PLL-g-PMOXA and PLL-g-PMOXA-c-FA. Finally, the carboxyl-terminated PMOXA−OH and PMOXA-*c*-FA were grafted onto PLL-HBr in PB using water-soluble carbodiimide chemistry as before.[19,31,32] To obtain PLL-*g*-PMOXA and PLL-*g*-PMOXA-*c*-FA with different FA functionality ratios, PMOXA−OH of decreasing amounts (90, 72, 54, 36, 18, 0 mg; or 0.030, 0.024, 0.018, 0.012, 0.006, 0 mmol) and PMOXA-*c*-FA of increasing quantities (0, 29, 59, 88, 118, 147 mg; or 0, 0.006, 0.012, 0.018, 0.024, 0.030 mmol) were mixed with PLL.HBr (21 mg, 0.10 mmol lysine residues), EDC-HCl (69 mg, 0.36 mmol) and Sulfo-NHS (6.5 mg, 0.030 mmol), and then dissolved in 3 mL PB. The solutions were maintained at agitation for 16 h and then purified by dialysis (12−14 000 MWCO tubing, Spectra/Por4, Spectrum Laboratories, Inc.) against ultrapure water (1 L × 8) for 2 days. The polymers were collected as white or yellow to orange powder with yields of ~80% after lyophilization. The chemical structures of the polymers were determined by ^{1}H NMR spectroscopy.

2.2. Characterization of Polymers. *2.2.1. Molecular Weight and Distribution By GPC.* The molecular weights of polymers were determined by gel permeation chromatography (GPC) using TSKgel G3000PWX column (Tosoh Biosep, Japan) on Waters 2695 Separation Module connected to a Waters 2414 refractive index detector. Samples were dissolved (1 mg/mL) in 0.1 M $NaNO_3$ solution as recommended by the manufacture of column and eluted with it at a rate of 1 mL/min. PEG (Cat. No.: 81288, 81290, 81293; $\bar{M}_n$ = 1000, 2000, 6000 g/mol; Fluka) was used as reference standard for calibration, and triplicate experiments were performed for each sample.

2.2.2. Chemical Structure by ^{1}H NMR Spectroscopy. Polymer solids were dissolved in D_2O (Cat. No.: 151882, Sigma-Aldrich) to the concentration of 5 to 10 mg/mL, of which ^{1}H NMR spectra were determined on a Bruker Avance II 400 MHz NMR Spectrometer. Each sample was scanned at least 64 times to get a high signal-to-noise (SNR) ratio. The spectra were calibrated by designating the chemical shift (δ) of HOD to be 4.8 ppm.

2.3. Preparation of Polymer Monolayers on Glass Wafers. Glass wafers (Yaohua Glass Ltd., Suzhou, China, 1 × 1 cm) were washed with piranha solution (30% H_2O_2/95% H_2SO_4 = 1:3) for 2 h, followed by ultrasonication in deionized (DI) water (5 min × 4). Subsequently, the wafers were blow-dried with nitrogen gas and cleaned by oxygen plasma (plasma cleaner/sterilizer PDC-32G, Harrick Scientific Products, Inc.) for 2 min. Polymer monolayers were prepared on the glass wafers using the dip-and-rinse protocol.[19,20,31,32] Briefly, each freshly prepared glass wafer was fully covered by 40 μL of polymer solution (4 μM in PB) for 3 h, followed by extensive rinsing with DI water and blow-dried with nitrogen gas again. The newly polymer-coated glass wafers were used for characterization or cell adhesion test immediately. As controls, PLL-coated (covered with 4 μM PLL in PB) and bare (covered with PB exclusively) glass wafers were also investigated.

2.4. Characterization of Polymer Monolayers on Glass Wafers. *2.4.1. Water Contact Angle and Zeta Potential Measurements.* Static water contact angle measurement was performed on a

DOI: 10.1021/am508399w
ACS Appl. Mater. Interfaces 2015, 7, 2919−2930

digital microscope platform (VHX-1000, Keyence Corporation, Itasca, IL). For each measurement ~5 μL of DI water was deposited onto the substrate and image was taken with a 20× objective along the plane of it. The contact angle was determined by a built-in software of the platform.

Zeta potential (ζ), which is an important parameter to characterize the charged solid−liquid interface, was determined by measuring the streaming current I_{str} induced by slip motion of diffuse counterions in the electrical double layer. When an aqueous solution (dielectric constant ε, density ρ) flows through (volume flow rate Q) a capillary (inner radius r), it will generate streaming current (I_{str}) and zeta potential can be calculated by the equation below:[52]

$$\zeta = -\frac{r^2}{8\varepsilon Q} I_{str} \quad (1)$$

Glass capillaries (D_{in} = 0.29 mm, Cat. No.: 1B100−4, World Precision Instruments Inc., Sarasota, FL) were immobilized with our polymers (4 μM in PB, 3 h) after being washed with piranha solution and rinsed with ultrapure water. Subsequently, mechanical syringe pump (PHD 2000, Harvard Apparatus, Holliston, MA) was used to precisely drive ultrapure water flow (Q from 100 to 600 mL/h, ε = 6.933×10^{-10} F/m) through a capillary, the ends of which were tightly joined by Ag/AgCl electrodes.[53] Streaming current was measured by a pico-ammeter (Model 487, Keithley Instruments, Inc., Cleveland, OH).

2.4.2. Time-of-Flight Secondary Ion Mass Spectrometry (ToF-SIMS) and Principle Component Analysis (PCA). ToF-SIMS was performed on a ToF-SIMS V spectrometer (Ion-ToF GmbH, Germany). The polymer monolayers (200 × 200 μm surface area) were bombarded with a Bi_3^+ beam at 25 keV in a 1.5×10^{-9} mbar vacuum at ambient temperature. The total ion dose is below 4×10^{11} ions/cm^2, thus meeting the criteria of static ToF-SIMS. Mass spectra with a high resolution ($m/\Delta m$) of ~8000 at the mass-to-charge ratio (m/z) of 29 ($C_2H_5^+$) were recorded on monolayers (duplicate experiments on three samples for each type). Positive mass spectra were investigated, which were calibrated using fragments H^+, CH_3^+, $C_2H_3^+$, and $C_3H_5^+$ with m/z of 1, 15, 27, and 41, respectively. The ion intensities were calculated by integral of the peak areas with the aid of IonSpec software. The selected ions were those with m/z ranges from 1 to 500 and with intensities above 10 counts. PCA was performed on positive fragments with the intensity of each peak normalized to the total sum of peak intensities for each measurement so that the data were independent of the intensity of primary ion source. A homemade program for PCA had been developed in Matlab R2013b (MathWorks, Inc., Natick, MA), of which the code was given in the Supporting Information.

2.5. Cell Attachment Test. *2.5.1. Cell Culturing and Harvesting.* HeLa (Human cervix adenocarcinoma cell line, CCL-2, ATCC), HeLa-C3,[54] MCF-7 (Human breast adenocarcinoma cell line, HTB-22, ATCC), JEG-3 (Human placental choriocarcinoma cell line, HTB-36, ATCC), and HepG2 (Human hepatocellular carcinoma cell line, HB-8065, ATCC) were used in this study. HeLa and HepG2 were cultured in high-glucose Dulbecco's modified Eagle's medium (DMEM; Cat. No.: D7777, Sigma-Aldrich) supplemented with 3.7 g/L $NaHCO_3$, 10% fetal bovine serum (FBS; Cat. No.: 26140−079, Life Technologies) and 1% penicillin/streptomycin (Cat. No.: 15140, Life Technologies). Other cell lines were raised in Eagle's minimal essential medium (EMEM) (Cat. No.: 61100-061, Life Technologies) supplemented with 1.5 g/L $NaHCO_3$, 10% FBS and 1% penicillin/streptomycin. The cells were maintained in culture dishes (60.1 cm^2, Cat. No.: 93100, TPP) with 10 mL medium at 37 °C with 5% CO_2 and the medium was renewed every other day. Cells were harvested when ~80% confluence had been reached. To harvest the cells, the medium was replaced by 5 mL phosphate buffered saline (PBS; 137 mM NaCl, 2.7 mM KCl, 10 mM Na_2HPO_4, 1.8 mM KH_2PO_4, pH = 7.4). After 5 min in the incubator, PBS was removed, 1 mL 0.05% trypsin (Cat. No.: 0458, Amresco) with 0.53 mM ethylenediaminetetraacetic acid disodium salt (EDTA.2Na, Cat. No.: LE118, Genview) (trypsin/EDTA.2Na) solution was added, and the cells were placed back in the incubator again until thoroughly detached with gentle shake. Subsequently, 9 mL of medium was added and the cells were either used for passage or for attachment test.

2.5.2. Adhesion and Spreading of HeLa and MCF-7 Cells on Various Substrates. Freshly prepared bare and polymer-coated glass wafers were placed into 24-well plates (Cat. No.: 92024, TPP, Switzerland) prior to use. After being rinsed with PBS, each wafer was seeded with 50 000 HeLa or MCF-7 cells in 1 mL of medium, and the cells were maintained at 37 °C with 5% CO_2 for 1 to 24 h. At designated time points, the medium was replaced by Hochest 33342 (Cat. No.: H1399, Ex/Em: 350/461 nm, Life Technologies, diluted to 2 μg/mL in PBS). After a nucleus staining period of 30 min, the solution was changed to PBS in succession with a single gentle washing with it. Cell nuclei were observed under an upright epifluorescence microscope (BX41, Olympus). Fluorescence images were taken with a computerized charge-coupled device (CCD) camera (12.0 Monochrome w/o IR-18, Diagnostic Instruments). To study cell spreading on various substrates, we further fixed the samples with paraformaldehyde (Cat. No.: P6148, Sigma-Aldrich, 4% in PBS) for 30 min, permeabilized with Triton X-100 (Cat. No.: T8787, Sigma-Aldrich, 0.1% in PBS) for 30 min, and then blocked with BSA (Cat. No.: A2153, Sigma-Aldrich, 5% in PBS) for 1 h. F-actin of cells was stained with Alexa Fluor 488-labeled phalloidin (Cat. No.: A12379, Ex/Em: 495/518 nm, Life technologies, diluted to 1 unit/mL in PBS). After a staining period of 1 h, the solution was changed to PBS in succession with double gentle washing with it. Cell nuclei and cytoskeleton were studied with an inverted fluorescent microscope (Eclipse TE2000-U, Nikon). Fluorescence images were recorded with a computerized CCD camera (7.2 Color Mosaic, Diagnostic Instruments) again. ImageJ (NIH) was used for counting cell nuclei and measuring the area of F-actin.

2.5.3. Influence of Free FA in the Medium on the Adhesion of HeLa cells. HeLa cells were resuspended in DMEM with additional free FA from 100 μM to 10 mM after detachment by the trypsin/EDTA.2Na solution. (The lower limit of 100 μM was set based on the formulation of medium, which contained 10 μM free FA.) Glass wafers immobilized with FA(0.91) or PLL (positive control) were seeded with 50 000 cells in 1 mL medium each and the cells were maintained at 37 °C with 5% CO_2 for 1 h. Subsequently, the cell nuclei were stained and analyzed as in section 2.5.2.

2.5.4. Influence of FA Functionality Ratio of PLL-g-PMOXA-c-FA on the Adhesion of HeLa Cells. Glass wafers coated with PLL-*g*-PMOXA-*c*-FA of various FA functionality ratios, PLL-*g*-PMOXA (negative control), or PLL (positive control) were seeded with 50 000 cells in 1 mL DMEM each, and the cells were maintained at 37 °C with 5% CO_2 for 1 h. Afterward, the cell nuclei were stained and analyzed as described in section 2.5.2.

2.5.5. Adhesion of JEG-3 and HepG2 Cells on Various Substrates. Freshly prepared bare and polymer-coated glass wafers were seeded with 50 000 JEG-3 or HepG2 cells in 1 mL of medium each, and the cells were maintained at 37 °C with 5% CO_2 for 1 or 3 h. Afterward, the cell nuclei were stained and analyzed as described in section 2.5.2.

2.6. Recovery of HeLa Cells from Mixture with MCF-7 Cells. Glass Petri dishes (D_{in} = 5 cm, Rutka Laborberdarf GmbH, Winklarn, Germany) were cleaned in the same way as glass wafers before and then fully covered with 1 mL FA(0.91) (experiment group, 4 μM in PB) or PLL (control group, 4 μM in PB) solution for 3 h. Subsequently, they were extensively rinsed with DI water and blow-dried with nitrogen gas. MCF-7 suspension was spiked with HeLa-C3 (green fluorescent protein (GFP)-transfected; 100:1) and seeded on the dishes at a density of 50 000 cells/cm^2. After at 37 °C with 5% CO_2 for 1 h, the medium was replaced by Hochest 33342 (2 μg/mL in PBS) for 15 min. The cells were then gently rinsed with PBS three times and observed under the upright epifluorescence microscope. Fluorescence images were taken and analyzed with ImageJ.

2.7. Statistical Study. Statistical significance was calculated by Welch's *t*-test for unpaired comparison with unequal variances. The analyses were performed with a homemade program in Matlab R2013b.

DOI: 10.1021/am508399w
ACS Appl. Mater. Interfaces 2015, 7, 2919−2930

Scheme 1. Schematic Illustration of the Preparation of PLL-*g*-PMOXA-*c*-FA[a]

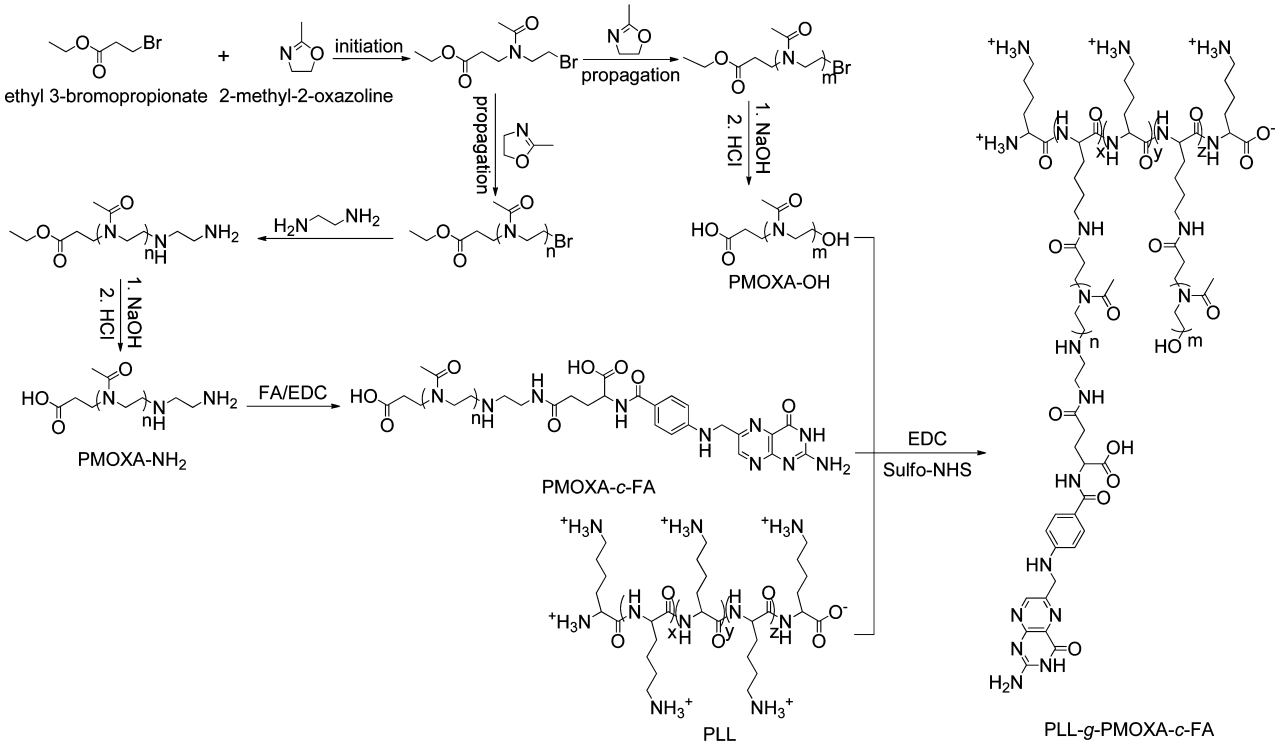

[a]PMOXA was synthesized by living cationic ring-opening isomerization polymerization using ethyl 3-bromopropionate as the initiator, through which carboxyl group could be introduced after hydrolysis at one end of the polymer. Longer chains of PMOXA-*c*-FA and shorter chains of PMOXA−OH were grafted onto PLL backbone via carbodiimide chemistry so that FA could have a better chance to interact with FR.

3. RESULTS AND DISCUSSION

3.1. Synthesis of PLL-*g*-PMOXA-*c*-FA. Previous studies have used methyl trifluoromethylsulfonate (MeOTf) to initiate the cationic ring-opening isomerization polymerization of MOXA.[19,31,32] However, using this initiator, one can only get monofunctional PMOXA so as to graft it onto a surface or another polymer for the antifouling purpose. To prepare bifunctional PMOXA for the goal of conjugating a bioactive molecule at the other end of it, one must use an initiator that could introduce anther functional group. Because of that, we utilized ethyl 3-bromopropionate instead of MeOTf (Scheme 1). The ester group from this initiator was hydrolyzed to the carboxyl group at one end of PMOXA. The bromine atom at the other end was replaced by a hydroxyl group or an amine group via nucleophilic reaction. The amine-functionalized PMOXA was used for the conjugation of FA so that two types of PMOXAs, FA-coupled PMOXA (PMOXA-*c*-FA) and hydroxyl-ended PMOXA (PMOXA−OH), were synthesized for the preparation of PLL-*g*-PMOXA-*c*-FA. The number-averaged molecular weight ($\bar{M}_n$) of PMOXA-*c*-FA and PMOXA−OH were around 4900 g/mol (PDI, 1.31) and 3000 g/mol (PDI, 1.20), respectively, as determined by gel permeation chromatography (GPC; Figure S1, Supporting Information). Longer chains of PMOXA-*c*-FA and shorter chains of PMOXA−OH were grafted onto PLL backbone via carbodiimide chemistry so that FA could have a better chance to interact with FR. PLL-*g*-PMOXA-*c*-FAs with varying FA functionality ratios at the side chain ends were prepared by adjusting the molar proportions of PMOXA-*c*-FA and PMOXA−OH. Table 1 summarized the polymers studied in this work. The grafting density and FA functionality ratio were calculated based on ^{1}H NMR spectra (FigureS2, Supporting Information).

Table 1. Summary of the Structural Characteristics of the Polymers

polymer	abbreviation	grafting density[a]	FA functionality ratio[b]
PLL[c]	PLL	0	0
PLL-*g*-PMOXA	PMOXA	0.29 ± 0.02	0
PLL-*g*-PMOXA-*c*-FA(0.18)	FA(0.18)	0.27 ± 0.02	0.18 ± 0.02
PLL-*g*-PMOXA-*c*-FA(0.36)	FA(0.36)	0.26 ± 0.03	0.36 ± 0.03
PLL-*g*-PMOXA-*c*-FA(0.54)	FA(0.54)	0.26 ± 0.03	0.54 ± 0.04
PLL-*g*-PMOXA-*c*-FA(0.74)	FA(0.74)	0.27 ± 0.03	0.74 ± 0.06
PLL-*g*-PMOXA-*c*-FA(0.91)	FA(0.91)	0.24 ± 0.02	0.91 ± 0.07

[a]The grafting density is defined as the proportion of conjugated lysine units. [b]The FA functionality ratio is defined as the proportion of PMOXA side chains with FA cap. [c]The number-averaged molecular weight of PLL is 21 000 g/mol (PDI = 1.04).

3.2. Characterization of Polymer Monolayers on Glass Wafers. *3.2.1. Water Contact Angle and Zeta Potential.* With a simple dip-and-rinse approach, the polymers were coated on clean glass wafers in our study.[19,20,31,32] Previous works have demonstrated that a dense brush-like monolayer could be spontaneously formed on negatively charged substrates induced by the electrostatic interaction between the surface and the PLL backbone.[32,55−57] The static water

DOI: 10.1021/am508399w
ACS Appl. Mater. Interfaces 2015, 7, 2919−2930

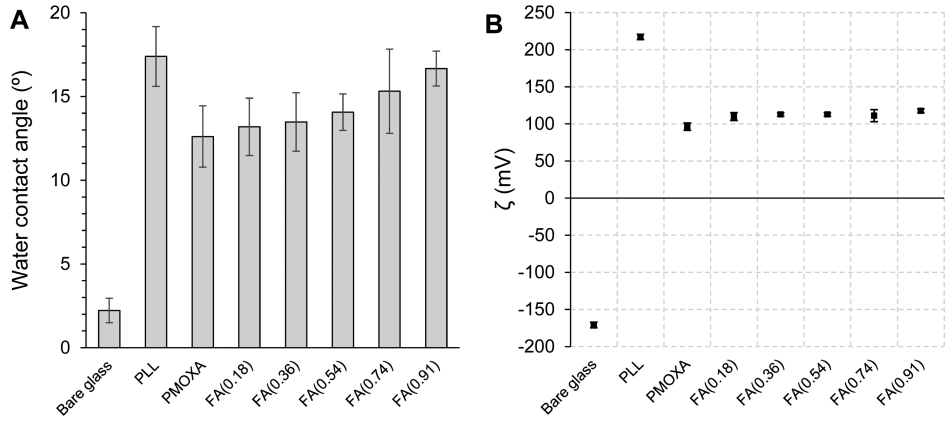

Figure 1. (A) Water contact angles (mean ± std, n = 9) and (B) zeta potentials (ζ) (mean ± std, n = 5) on various substrates.

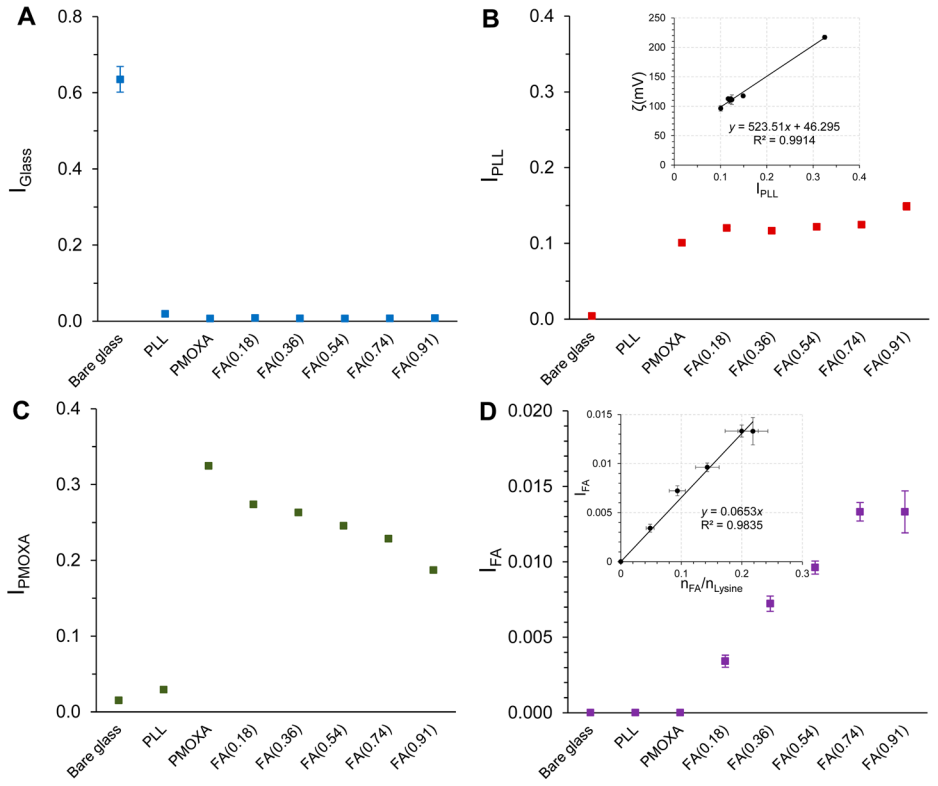

Figure 2. ToF-SIMS and PCA: the normalized total intensity of positive characteristic secondary ions assigned to (A) bare glass, (B) PLL, (C) PMOXA, and (D) FA on various substrate (mean ± std, n = 6). (B, inset) Positive and linear relationship between the zeta potential and the intensity of PLL-related fragments for the glass surfaces coated with polymers; (D, inset) positive and proportional relationship between the intensity of FA-related fragment and the molar ratio of FA caps over L-lysine residues (n_{FA}/n_{Lysine}) of PLL backbone.

contact angle and zeta potential on glass surfaces immobilized with different polymers were determined (Figure 1). Our results showed that all polymer-coated surfaces were highly hydrophilic with contact angles below 20° and the values of bare glass and PLL- and PLL-*g*-PMOXA-coated glass were in agreement with those published previously.[32] A slight decrease of hydrophilicity with the increase of FA functionality ratio was observed. This could be explained by the hydrophobic nature of FA, which is almost insoluble in water at its molecular state.[58] The zeta potentials of PLL-*g*-PMOXA-*c*-FA-coated glass (110−120 mV) were slightly higher than that of PLL-*g*-PMOXA-coated one (96 mV) and in stark contrast to that of bare glass (−171 mV). Compared to the value of PLL-coated glass surface (217 mV), the zeta potentials of PLL-*g*-PMOXA-*c*-FA-coated ones decreased nearly by half, indicating the neutral nature and shielding effect of PMOXA.

3.2.2. ToF-SIMS and PCA. The surface chemistry of the substrates was further investigated by static ToF-SIMS. The principle for PCA in the analysis of ToF-SIMS data is discussed in published literatures[57,59] and is also briefly introduced in the Supporting Information. The scores of the first- and second-principal components proved to be sufficient to reflect the main features of those peaks, which together captured 97.9% of variance (Figure S3, Supporting Information). Characteristic fragments were selected out according to their loadings (absolute loading value >0.1 except for the one related to FA, Figure S4 and Table S1, Supporting Information) and assigned to the bare glass, PLL, PMOXA, or FA based on their structures

DOI: 10.1021/am508399w
ACS Appl. Mater. Interfaces 2015, 7, 2919−2930

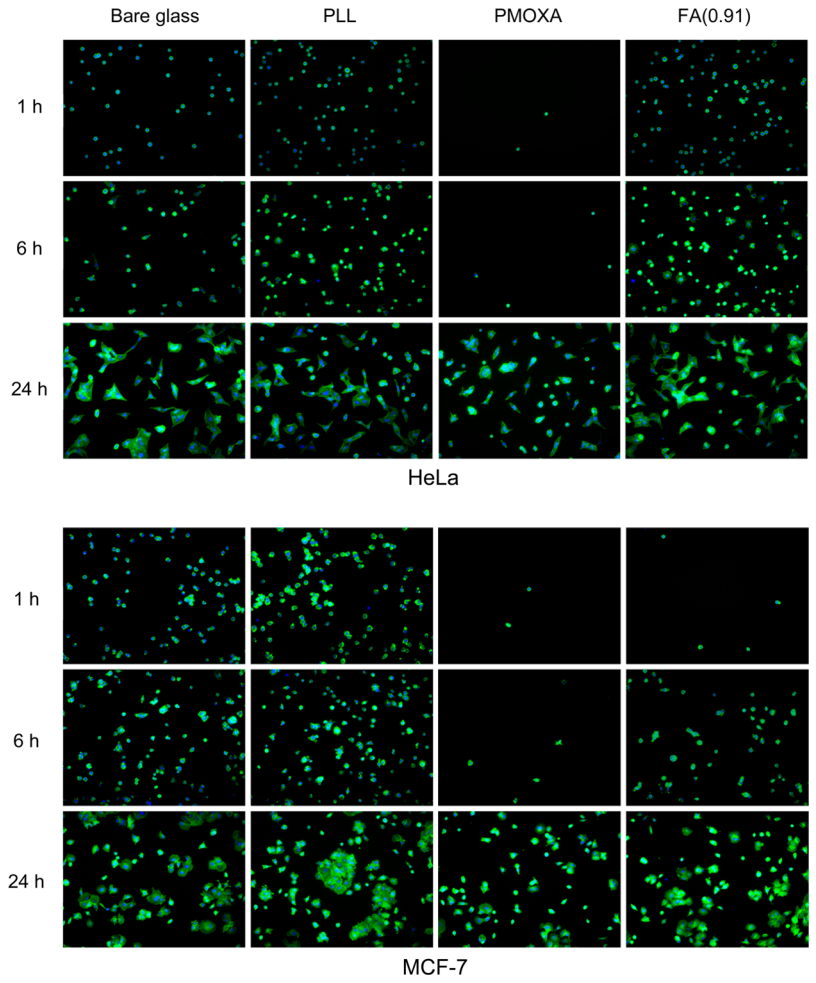

Figure 3. Fluorescence images showing the adhesions and spreading of HeLa and MCF-7 cells on various substrates at different time points; (blue) cell nuclei stained by Hochest 33342, (green) cell F-actin stained by Alexa Fluor 488-labeled phalloidin.

and relative intensities from different substrates, which were then summed up by assignments (Figure 2). It can be seen that the bare glass-related fragments were negligible after the surfaces had been covered with polymer solutions (Figure 2A), suggesting the successful immobilization of polymer layers. There were almost no PLL- and PMOXA-related fragments on bare glass surface, corroborating the neatness of it before coating. Compared to PLL-coated glass, the intensities of PLL-related fragments on the copolymer-coated ones decreased dramatically. For FA(0.18) to FA(0.74), the intensities of PLL-related fragments were approximately the same, while for PMOXA and FA(0.91) they were slightly lower and higher, respectively. The reduction of PLL-related fragments on the copolymer-modified substrates suggested the protection against the fragmentation of L-lysine residues by PMOXA side chains. It is worthwhile to note that the zeta potential of polymer-coated glass surfaces was linearly and positively correlated to the intensity of PLL-related fragments for the polymers used in this study, as revealed by the inset in Figure 2B, confirming the polycationic nature of PLL. The intensity of PMOXA-related fragments decreased with the increment of FA functionality ratio, which implied that FA caps protected PMOXA side chains from fragmentation to some extent (Figure 2C). Although with much smaller amounts compared to other components, FA-related fragment could be readily detected by ToF-SIMS as well (Figure 2D). The intensity of it, which reflected the density of conjugated FA on the substrates, increased with the increment of FA functionality ratio from 0 to 0.74, while no significant difference was observed between FA(0.74) and FA(0.91)-coated glass surfaces. However, as the grafting density on PLL backbone of FA(0.91) was smaller than those of other copolymers, the molar ratio of FA caps over L-lysine residues (n_{FA}/n_{Lysine}) would be more accurate to reflect the structural characteristics of the copolymers. Our results demonstrated that the intensity of FA-related fragment was nearly proportional to n_{FA}/n_{Lysine} (Figure 2D, inset).

3.3. Cell Attachment Test. *3.3.1. Adhesion and Spreading of HeLa and MCF-7 Cells on Various Substrates.* As mentioned above, our materials were developed for specific targeting to some cancer cells. It is hypothesized that PLL-*g*-PMOXA-*c*-FA-immobilized glass surface would be adhesive to FR-positive cancer cells while anti-adhesive to FR-negative cells. On the basis of this hypothesis, we investigated the adhesion and spreading of two types of cancer cell lines HeLa (FR-positive) and MCF-7 (FR-negative) on FA(0.91)-coated glass with bare glass, PLL-coated glass, and PLL-*g*-PMOXA-coated glass as controls. The results are displayed in Figures 3 and 4. It is noted that the cell behaviors could be divided into two stages, cell-adhesion stage (within 3 h) and cell-spreading stage (after 3 h). During the cell-adhesion stage, there was hardly any spreading of cells involved, and it was observed that most of the cells attached onto PLL-coated glass surface for

DOI: 10.1021/am508399w
ACS Appl. Mater. Interfaces 2015, 7, 2919−2930

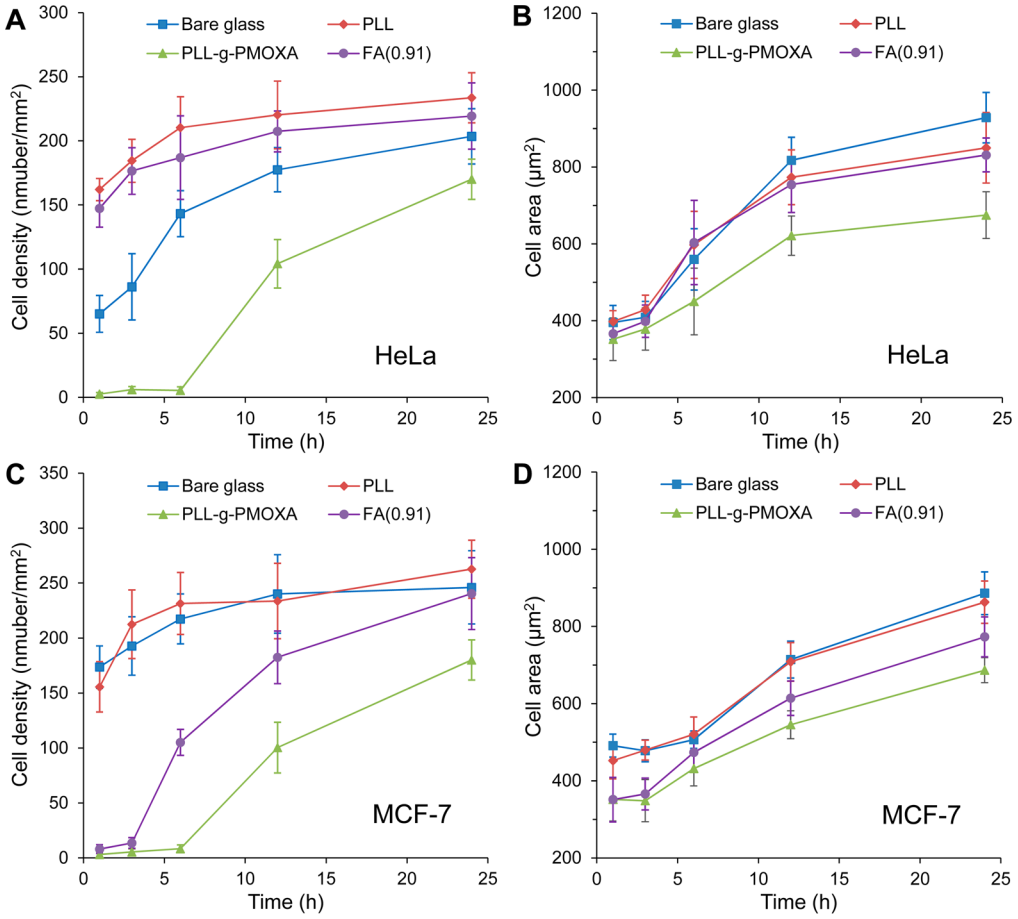

Figure 4. Quantitative study of cell behaviors on various substrates. (A and B) Adhesion and spreading of HeLa cells on the substrates as functions of time (mean ± sem, n = 9 from triplicate experiments). (C and D) Adhesion and spreading of MCF-7 cells on the substrates as functions of time (mean ± sem, n = 9 from triplicate experiments).

both cell lines. However, the adhesions of HeLa and MCF-7 cells were dramatically different on FA(0.91)-coated glass within this period. While the cell density of HeLa on FA(0.91)-coated glass was nearly the same as that on PLL-coated glass, few MCF-7 cells were found to attach onto FA(0.91)-coated glass, indicating a specific interaction existed between the biorecognition moiety and the cell receptor. Interestingly, it was noted that the cell density on bare glass surface was almost as half as that on PLL-coated surface for HeLa but comparable for MCF-7 during this stage, suggesting glass surface was much less adhesive to HeLa than to MCF-7 at the beginning. As expected, only few cells attached onto PLL-*g*-PMOXA-coated glass for both types of cells, proving the excellent anti-adhesive property of PMOXA. As cells entered the spreading stage, they started to expand with great variations on different substrates.

The densities of both types of cells continued to increase on all the substrates, among which PLL-coated glass exhibited the best adhesiveness. For HeLa cells, the growth of population on FA(0.91)-immobilized glass was nearly comparable as that on PLL-modified one and most of the cells seeded on bare glass adhered after 6 h. Interestingly, the cells on bare glass reached a density a little bit lower than those on PLL- or FA(0.91)-coated glass surface after 24 h. The dramatic increment in affinity of bare glass to HeLa cells with culturing time was likely due to the modification of glass surface by deposition of proteins in cell medium or secreted by cells. The spreading of HeLa cells was similar at early spreading stage (6 h) on bare glass and on PLL- and FA(0.91)-modified substrates but then became greater on bare glass, which could be explained by the crowdedness of cells on the other two substrates as indicated by the higher cell densities. For MCF-7, the bare glass showed almost identical adhesiveness as the PLL-coated glass from perspectives of both the cell density and spreading. Although FA(0.91)-modified substrate was bioinert to MCF-7 cells at the adhesion stage, it gradually lost its antifouling property. Nearly half of the cells adhered on this substrate after 6 h, and the density of them was even as large as those on the bare glass or PLL-coated one at the end of the test (24 h after seeding), unlike their floating state within the initial 3 h in which the cells could be readily removed by aspiration of the medium. This could be explained by the noncovalent nature of the electrostatic interaction between glass surface and PLL backbone, and a similar phenomenon was also observed for PLL-*g*-PMOXA, which gradually lost its bioinert function to both HeLa and MCF-7 after 6 h. A previous study has demonstrated that SiO_2-based substrate has smaller negative charge density compared to some metal oxide-based substrates such as Nb_2O_5,[50] resulting in less PLL-*g*-PMOXA adsorbed onto the glass surface and weaker electrostatic interaction between them. Because of that, the brush-like polymer layer could have been replaced by the proteins in medium or secreted by cells, and the surface eventually became adhesive to cells.

DOI: 10.1021/am508399w
ACS Appl. Mater. Interfaces 2015, 7, 2919−2930

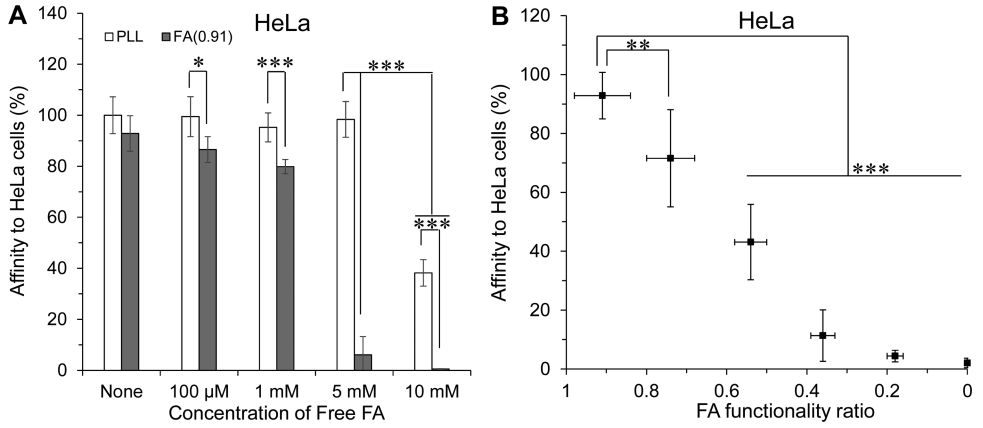

Figure 5. (A) Affinity of FA(0.91)-coated glass to HeLa as a function of concentration of free FA and (B) affinity of PLL-*g*-PMOXA-*c*-FA-coated glass to HeLa as a function of FA functionality ratio (mean ± sem, $n = 9$ from triplicate experiments). Samples were harvested 1 h after the cells had been seeded, and affinity was defined as the ratio of cell density on a specific substrate over that on the PLL-coated glass in percentage. (*) $P < 0.05$; (**) $P < 0.01$; (***) $P < 0.001$).

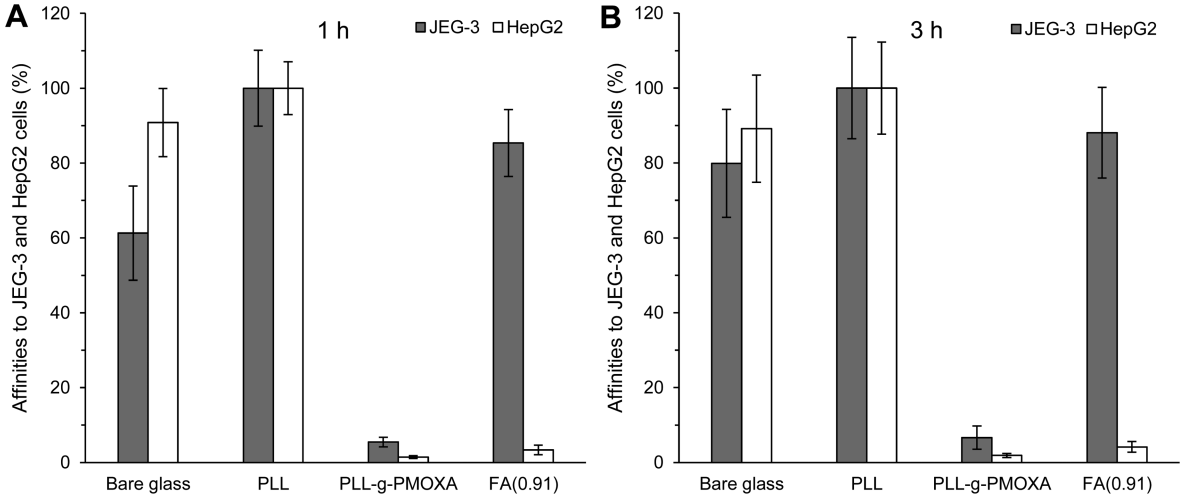

Figure 6. Affinities of various substrates to JEG-3 and HepG2 cells after (A) 1 h and (B) 3 h. Affinity was defined as the ratio of cell density on a specific substrate over the cell density on the PLL-coated glass in percentage (mean ± sem, $n = 9$ from triplicate experiments).

3.3.2. Influence of Free FA in the Medium on the Adhesion of HeLa Cells. To corroborate the specific interaction between FA and FR on HeLa cells, we added free FA to the cell culture medium to test its inhibition on cell adhesion on FA(0.91)-coated glass. PLL-coated glass was used as a control. Unlike a study in which the binding affinity of FA-coupled PEG to FR-positive cells was thoroughly inhibited when the concentration of free FA was just on the scale of 100 μM,[60] our study found that the adhesion of HeLa cells on FA(0.91)-coated glass was not efficiently suppressed until the concentration of it reached 5 mM (Figure 5A). Up to this concentration, no suppression of cell adhesion on PLL-coated glass was observed. Further increase of free FA not only thoroughly inhibited the adhesion of HeLa on FA(0.91)-coated glass, but also restrained that on PLL-coated glass, probably due to the reduced viability of cells at such high concentration. These results validated that the specific interaction between FR on cell membrane and conjugated FA played a decisive role in the attachment of HeLa on FA(0.91)-coated glass in the beginning. The results also implied that FA(0.91)-modified glass surface had such a high density of conjugated FA that even under inhibition of high concentration of free FA, it still had a good chance to bind to HeLa cells due to the multivalent nature of the interaction between FA and FR on the cells, which was consistent with other studies.[60,61]

3.3.3. Influence of FA Functionality Ratio of PLL-g-PMOXA-c-FA on the Adhesion of HeLa Cells. As FA has shown a specific interaction with FR, another important issue is the effect of the surface density of FA on this interaction. To elucidate this, we synthesized PLL-*g*-PMOXA-*c*-FAs with smaller FA functionality ratios as mentioned before and immobilized on the glass surface to test their affinity to HeLa cells. Our results (Figure 5B) demonstrated that the affinity of PLL-*g*-PMOXA-*c*-FA-coated surface to HeLa cells declined dramatically with the reduction of FA functionality ratio. At first glance, it seemed the affinity of the substrates to HeLa was mainly affected by the surface density of conjugated FA as prior analysis on ToF-SIMS indicated that it decreased with the reduction of FA functionality in a general trend. However, it was noted that FA(0.91)-coated surface showed significantly higher affinity to HeLa than that shown by FA(0.74)-modified surface ($P < 0.01$), while the surface density of FA was almost the same between them. As FA(0.74) had more PMOXA−OH side chains on PLL backbone than FA(0.91), these observations suggested the affinity of the copolymer-coated substrates to HeLa was more affected by PMOXA−OH than

DOI: 10.1021/am508399w
ACS Appl. Mater. Interfaces 2015, 7, 2919−2930

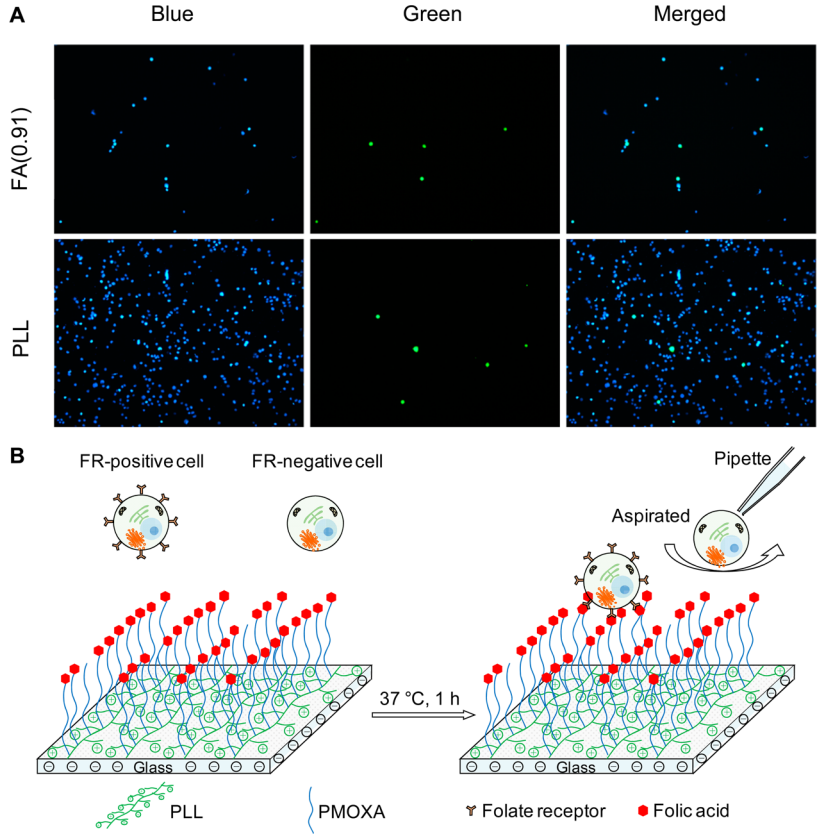

Figure 7. (A) Fluorescence images showing the recovery of HeLa cells from the mixture with MCF-7 on FA(0.91)-modified and PLL-modified glass surfaces. HeLa cells were transfected with green-fluorescent protein gene;[54] (blue) cell nuclei of both HeLa and MCF-7 and (green) HeLa cells. (B) Proposed structure of PLL-*g*-PMOXA-*c*-FA on glass surface and the principle for the recovery of FR-positive cancer cells. FR-positive cells were captured by the specific interaction, while FA-negative cells were repelled by the antifouling PMOXA chains in 1 h.

PMOXA-*c*-FA side chains. Gabizon et al.,[60] reported that the binding affinity of PEG-*c*-FA-grafted liposome to FR was significantly impaired when the liposome contained methoxyl PEG (mPEG) with the same molecular weight (2000 g/mol) as the PEG tether of PEG-*c*-FA but was not affected much when higher molecular weight of PEG tether (3400 g/mol) was used. On the basis of their results and ours, it can be concluded that once immobilized on a substrate, hydroxyl- or methoxyl-terminated antifouling polymer chains can block the specific interaction between targeted receptors on a cell and targeting moieties on the surface, unless the tethering antifouling polymer chains of them are longer. In fact, that was the rationale for the design of our copolymers, based on which longer PMOXA-*c*-FA (4900 g/mol) and shorter PMOXA−OH (3000 g/mol) were synthesized and grafted onto PLL. However, due to the polydispersity of the polymers, the interaction between FA and FR was still severely inhibited by PMOXA−OH, as reflected by the low binding affinity (4.4 ± 1.9%) of FA(0.18)-modified substrate to HeLa compared to that of FA(0.91) (92.9 ± 7.9%). Nonetheless, it is believed that the inhibitory effect of PMOXA−OH on this specific interaction could be eliminated as long as much longer chains of PMOXA-*c*-FA or polymers with much better uniformity (i.e., much smaller PDI) are to be used.

3.3.4. Adhesion of JEG-3 and HepG2 Cells on Various Substrates. To understand whether this interaction was cell-type dependent, we investigated the behaviors of two other types of cells, JEG-3 (placental choriocarcinoma cell line, FR-positive) and HepG2 (liver carcinoma cell line, FR-negative) on the substrates during cell adhesion stage.[45,62,63] Our results (Figure 6) revealed the behavior of JEG-3 was similar to that of HeLa, while the behavior of HepG2 was similar to that of MCF-7. On the basis of these results, we can conclude that the specific interaction between FA and FR is cell-type independent and should be universal to other kinds of FR-positive cancer cells.

3.4. Recovery of HeLa Cells from Mixture with MCF-7 Cells. So far, we have systematically studied the properties of the copolymers. We believe that our materials will have important applications in cancer-related areas, such as a targeted drug delivery system or as a substrate coating for the isolation of circulating tumor cells (CTCs). As a demonstration for the second application, we spiked MCF-7 cells with HeLa (100:1) and seeded them (50 000 cells/cm^2) on FA(0.91)- and PLL-modified surfaces. After 1 h, the unattached cells were removed, and we found markedly fewer MCF-7 cells adhered on FA(0.91)-modified surface than PLL-modified surface, while the densities of HeLa cells were close on those two substrates (Figure 7A). Although the specific interaction between FA(0.91)-coated glass and HeLa cells could only hold for 3 h, it was proved to be enough for recovering them from the mixture with MCF-7 cells due to the specific interaction between FA and FR (Figure 7B). Quantitative analysis revealed that more than 95.6 ± 13.3% of HeLa cells were recovered on FA(0.91)-modified surface (97.8 ± 12.0% for PLL-modified surface) and the proportion of HeLa cells increased drastically to 24.3 ± 8.6% (1.1 ± 0.2% for PLL-modified surface), demonstrating both high sensitivity and good specificity of

DOI: 10.1021/am508399w
ACS Appl. Mater. Interfaces 2015, 7, 2919−2930

FA(0.91)-modified substrate toward FR-positive cells, which is crucial for its applications in the future.

4. CONCLUSION

In summary, we have synthesized a novel bioactive copolymer using folic acid (FA) as the targeting moiety, poly(2-methyl-2-oxazoline) (PMOXA) as the tethering chain, and poly(L-lysine) (PLL) as the anchor. PLL backbone of this copolymer is positively charged at neutral aqueous solutions and could readily adsorb onto negatively charged substrates (such as clean glass surface in this study) by electrostatic interaction. The copolymer-coated glass surface was adhesive to folate receptor (FR)-positive cells (HeLa and JEG-3) but antifouling to FR-negative ones (MCF-7 and HepG2), corroborating the specific interaction between FA and FR, which was also confirmed by the inhibitory effect of free FA on it. In addition, the FA functionality ratio of it could be precisely regulated by the molar proportion of hydroxyl-ended PMOXA (PMOXA−OH, $\bar{M}_n$ = 3000 g/mol) and FA-coupled PMOXA (PMOXA-*c*-FA, $\bar{M}_n$ = 4900 g/mol) to be used during the synthesis. Our study revealed that the binding affinity of glass surface modified by it to HeLa was severely impaired by PMOXA−OH chains at low FA functionality ratios, which must be caused by polydispersity of the polymers. Nevertheless, it is believed that this inhibitory effect could be eliminated as long as much longer chains of PMOXA-*c*-FA or polymers with much better uniformity are used. In the end, we also demonstrated successful recovery of HeLa cells from a mixture with MCF-7 on the copolymer-coated glass. Future work on application of it as a targeted drug delivery system is in process now.

■ ASSOCIATED CONTENT

Ⓢ Supporting Information

GPC and 1H NMR data on various polymers, principle and additional results of PCA on ToF-SMIS data, and code for PCA in Matlab R2013b. This material is available free of charge via the Internet at http://pubs.acs.org.

■ AUTHOR INFORMATION

Corresponding Author

*E-mail: chhkwu@ust.hk.

Author Contributions

#These authors contributed equally to this work.

Notes

The authors declare no competing financial interest.

■ ACKNOWLEDGMENTS

This work was financially supported by the Theme-based Research Scheme (TBR), General Research Fund (GRF), and Collaborative Research Fund (CRF) from the Research Grant Council (RGC) of Hong Kong (Project No.: T13-706/11-2, GRF604712, and CUHK4/CRF/12G). W.W. also acknowledges support from the National Natural Science Foundation of China (NSFC)/Research Grants Council (RGC) Joint Research Scheme (Project No.: N_HKUST601/11). Y.C. gratefully appreciates Mrs. Eunice Yee-Lai Wang for her help with ^{1}H NMR measurement and Dr. Lutao Weng for his contribution in ToF-SIMS survey and analysis.

■ REFERENCES

(1) Yu, Q. A.; Zhang, Y. X.; Wang, H. W.; Brash, J.; Chen, H. Anti-Fouling Bioactive Surfaces. *Acta Biomater.* **2011**, *7*, 1550−1557.

(2) Zhen, G. L.; Eggli, V.; Voros, J.; Zammaretti, P.; Textor, M.; Glockshuber, R.; Kuennemann, E. Immobilization of the Enzyme Beta-Lactamase on Biotin-Derivatized Poly(L-lysine)-*g*-poly(ethylene glycol)-Coated Sensor Chips: A Study on Oriented Attachment and Surface Activity by Enzyme Kinetics and in Situ Optical Sensing. *Langmuir* **2004**, *20*, 10464−10473.

(3) Huang, N. P.; Voros, J.; De Paul, S. M.; Textor, M.; Spencer, N. D. Biotin-Derivatized Poly(L-lysine)-*g*-poly(ethylene glycol): A Novel Polymeric Interface for Bioaffinity Sensing. *Langmuir* **2002**, *18*, 220−230.

(4) Wolter, A.; Niessner, R.; Seidel, M. Preparation and Characterization of Functional Poly(ethylene glycol) Surfaces for the Use of Antibody Microarrays. *Anal. Chem.* **2007**, *79*, 4529−4537.

(5) Ameringer, T.; Hinz, M.; Mourran, C.; Seliger, H.; Groll, J.; Moeller, M. Ultrathin Functional Star PEG Coatings for DNA Microarrays. *Biomacromolecules* **2005**, *6*, 1819−1823.

(6) Schlapak, R.; Pammer, P.; Armitage, D.; Zhu, R.; Hinterdorfer, P.; Vaupel, M.; Fruhwirth, T.; Howorka, S. Glass Surfaces Grafted with High-Density Poly(ethylene glycol) as Substrates for DNA Oligonucleotide Microarrays. *Langmuir* **2006**, *22*, 277−285.

(7) Wach, J. Y.; Bonazzi, S.; Gademann, K. Antimicrobial Surfaces through Natural Product Hybrids. *Angew. Chem., Int. Ed.* **2008**, *47*, 7123−7126.

(8) Laloyaux, X.; Fautre, E.; Blin, T.; Purohit, V.; Leprince, J.; Jouenne, T.; Jonas, A. M.; Glinel, K. Temperature-Responsive Polymer Brushes Switching from Bactericidal to Cell-Repellent. *Adv. Mater.* **2010**, *22*, 5024−5028.

(9) Nagrath, S.; Sequist, L. V.; Maheswaran, S.; Bell, D. W.; Irimia, D.; Ulkus, L.; Smith, M. R.; Kwak, E. L.; Digumarthy, S.; Muzikansky, A.; Ryan, P.; Balis, U. J.; Tompkins, R. G.; Haber, D. A.; Toner, M. Isolation of Rare Circulating Tumour Cells in Cancer Patients by Microchip Technology. *Nature* **2007**, *450*, 1235−1239.

(10) Ma, Z. W.; Mao, Z. W.; Gao, C. Y. Surface Modification and Property Analysis of Biomedical Polymers Used for Tissue Engineering. *Colloids Surf., B* **2007**, *60*, 137−157.

(11) Schliephake, H.; Scharnweber, D. Chemical and Biological Functionalization of Titanium for Dental Implants. *J. Mater. Chem.* **2008**, *18*, 2404−2414.

(12) Gabizon, A.; Shmeeda, H.; Horowitz, A. T.; Zalipsky, S. Tumor Cell Targeting of Liposome-Entrapped Drugs with Phospholipid-Anchored Folic Acid-PEG Conjugates. *Adv. Drug Delivery Rev.* **2004**, *56*, 1177−1192.

(13) Kidane, A. G.; Salacinski, H.; Tiwari, A.; Bruckdorfer, K. R.; Seifalian, A. M. Anticoagulant and Antiplatelet Agents: Their Clinical and Device Application(s) together with Usages to Engineer Surfaces. *Biomacromolecules* **2004**, *5*, 798−813.

(14) Yuan, S. S.; Zhao, J.; Luan, S. F.; Yan, S. J.; Zheng, W. L.; Yin, J. H. Nuclease-Functionalized Poly(styrene-*b*-isobutylene-*b*-styrene) Surface with Anti-Infection and Tissue Integration Bifunctions. *ACS Appl. Mater. Interfaces* **2014**, *6*, 18078−18086.

(15) Banerjee, I.; Pangule, R. C.; Kane, R. S. Antifouling Coatings: Recent Developments in the Design of Surfaces That Prevent Fouling by Proteins, Bacteria, and Marine Organisms. *Adv. Mater.* **2011**, *23*, 690−718.

(16) Zhou, J. H.; Yan, H.; Ren, K. N.; Dai, W.; Wu, H. K. Convenient Method for Modifying Poly(dimethylsiloxane) with Poly(ethylene glycol) in Microfluidics. *Anal. Chem.* **2009**, *81*, 6627−6632.

(17) Branch, D. W.; Wheeler, B. C.; Brewer, G. J.; Leckband, D. E. Long-Term Stability of Grafted Polyethylene Glycol Surfaces for Use with Microstamped Substrates in Neuronal Cell Culture. *Biomaterials* **2001**, *22*, 1035−1047.

(18) Roosjen, A.; de Vries, J.; van der Mei, H. C.; Norde, W.; Busscher, H. J. Stability and Effectiveness Against Bacterial Adhesion of Poly(ethylene oxide) Coatings in Biological Fluids. *J. Biomed. Mater. Res., Part B* **2005**, *73B*, 347−354.

(19) Pidhatika, B.; Rodenstein, M.; Chen, Y.; Rakhmatullina, E.; Muhlebach, A.; Acikgoz, C.; Textor, M.; Konradi, R. Comparative Stability Studies of Poly(2-methyl-2-oxazoline) and Poly(ethylene glycol) Brush Coatings. *Biointerphases* **2012**, *7*, 1.

DOI: 10.1021/am508399w
ACS Appl. Mater. Interfaces 2015, 7, 2919−2930

(20) Chen, Y.; Pidhatika, B.; von Erlach, T.; Konradi, R.; Textor, M.; Hall, H.; Lühmann, T. Comparative Assessment of the Stability of Nonfouling Poly(2-methyl-2-oxazoline) and Poly(ethylene glycol) Surface Films: An in Vitro Cell Culture Study. *Biointerphases* **2014**, *9*, 031003.
(21) Mkhatresh, O. A.; Heatley, F. A Study of the Products and Mechanism of the Thermal Oxidative Degradation of Poly(ethylene oxide) Using 1H and 13C 1-D and 2-D NMR. *Polym. Int.* **2004**, *53*, 1336−1342.
(22) Pielichowski, K.; Flejtuch, K. Non-Oxidative Thermal Degradation of Poly(ethylene oxide): Kinetic and Thermoanalytical Study. *J. Anal. Appl. Pyrolysis* **2005**, *73*, 131−138.
(23) Holland, N. B.; Qiu, Y. X.; Ruegsegger, M.; Marchant, R. E. Biomimetic Engineering of Non-Adhesive Glycocalyx-like Surfaces Using Oligosaccharide Surfactant Polymers. *Nature* **1998**, *392*, 799−801.
(24) Zhang, X. Y.; Zhang, X. Q.; Yang, B.; Liu, M. Y.; Liu, W. Y.; Chen, Y. W.; Wei, Y. Facile Fabrication and Cell Imaging Applications of Aggregation-Induced Emission Dye-Based Fluorescent Organic Nanoparticles. *Polym. Chem.* **2013**, *4*, 4317−4321.
(25) Statz, A. R.; Meagher, R. J.; Barron, A. E.; Messersmith, P. B. New Peptidomimetic Polymers for Antifouling Surfaces. *J. Am. Chem. Soc.* **2005**, *127*, 7972−7973.
(26) Zhang, X. Q.; Liu, M. Y.; Yang, B.; Zhang, X. Y.; Wei, Y. Tetraphenylethene-Based Aggregation-Induced Emission Fluorescent Organic Nanoparticles: Facile Preparation and Cell Imaging Application. *Colloids Surf., B* **2013**, *112*, 81−86.
(27) Jiang, S. Y.; Cao, Z. Q. Ultralow-Fouling, Functionalizable, and Hydrolyzable Zwitterionic Materials and Their Derivatives for Biological Applications. *Adv. Mater.* **2010**, *22*, 920−932.
(28) Chang, Y.; Chang, W. J.; Shih, Y. J.; Wei, T. C.; Hsiue, G. H. Zwitterionic Sulfobetaine-Grafted Poly(vinylidene fluoride) Membrane with Highly Effective Blood Compatibility via Atmospheric Plasma-Induced Surface Copolymerization. *ACS Appl. Mater. Interfaces* **2011**, *3*, 1228−1237.
(29) Zhang, L.; Cao, Z. Q.; Bai, T.; Carr, L.; Ella-Menye, J. R.; Irvin, C.; Ratner, B. D.; Jiang, S. Y. Zwitterionic Hydrogels Implanted in Mice Resist the Foreign-Body Reaction. *Nat. Biotechnol.* **2013**, *31*, 553−556.
(30) Li, H. Y.; Zhang, X. Q.; Zhang, X. Y.; Yang, B.; Yang, Y.; Huang, Z. F.; Wei, Y. Zwitterionic Red Fluorescent Polymeric Nanoparticles for Cell Imaging. *Macromol. Biosci.* **2014**, *14*, 1361−1367.
(31) Konradi, R.; Pidhatika, B.; Muhlebach, A.; Textort, M. Poly-2-methyl-2-oxazoline: A Peptide-like Polymer for Protein-Repellent Surfaces. *Langmuir* **2008**, *24*, 613−616.
(32) Pidhatika, B.; Möller, J.; Benetti, E. M.; Konradi, R.; Rakhmatullina, E.; Muhlebach, A.; Zimmermann, R.; Werner, C.; Vogel, V.; Textor, M. The Role of the Interplay between Polymer Architecture and Bacterial Surface Properties on the Microbial Adhesion to Polyoxazoline-Based Ultrathin Films. *Biomaterials* **2010**, *31*, 9462−9472.
(33) von Erlach, T.; Zwicker, S.; Pidhatika, B.; Konradi, R.; Textor, M.; Hall, H.; Luhmann, T. Formation and Characterization of DNA-Polymer-Condensates Based on Poly(2-methyl-2-oxazoline) Grafted Poly(L-lysine) for Non-Viral Delivery of Therapeutic DNA. *Biomaterials* **2011**, *32*, 5291−5303.
(34) Obeid, R.; Scholz, C. Synthesis and Self-Assembly of Well-Defined Poly(amino acid) End-Capped Poly(ethylene glycol) and Poly(2-methyl-2-oxazoline). *Biomacromolecules* **2011**, *12*, 3797−3804.
(35) Guillerm, B.; Darcos, V.; Lapinte, V.; Monge, S.; Coudane, J.; Robin, J. J. Synthesis and Evaluation of Triazole-Linked Poly(epsilon-caprolactone)-graft-poly(2-methyl-2-oxazoline) Copolymers as Potential Drug Carriers. *Chem. Commun.* **2012**, *48*, 2879−2881.
(36) Bauer, M.; Schroeder, S.; Tauhardt, L.; Kempe, K.; Schubert, U. S.; Fischer, D. In Vitro Hemocompatibility and Cytotoxicity Study of Poly(2-methyl-2-oxazoline) for Biomedical Applications. *J. Polym. Sci., Part A: Polym. Chem.* **2013**, *51*, 1816−1821.
(37) Bai, L. C.; Tan, L.; Chen, L. J.; Liu, S. T.; Wang, Y. M. Preparation and Characterizations of Poly(2-methyl-2-oxazoline) Based Antifouling Coating by Thermally Induced Immobilization. *J. Mater. Chem. B* **2014**, *2*, 7785−7794.
(38) Hoogenboom, R.; Fijten, M. W. M.; Thijs, H. M. L.; Van Lankvelt, B. M.; Schubert, U. S. Microwave-Assisted Synthesis and Properties of a Series of Poly(2-alkyl-2-oxazoline)s. *Des. Monomers Polym.* **2005**, *8*, 659−671.
(39) Wiesbrock, F.; Hoogenboom, R.; Leenen, M. A. M.; Meier, M. A. R.; Schubert, U. S. Investigation of the Living Cationic Ring-Opening Polymerization of 2-Methyl-, 2-Ethyl-, 2-Nonyl-, and 2-Phenyl-2-oxazoline in a Single-Mode Microwave Reactor. *Macromolecules* **2005**, *38*, 5025−5034.
(40) Hoogenboom, R. Poly(2-oxazoline)s: A Polymer Class with Numerous Potential Applications. *Angew. Chem., Int. Ed.* **2009**, *48*, 7978−7994.
(41) Sedlacek, O.; Monnery, B. D.; Filippov, S. K.; Hoogenboom, R.; Hruby, M. Poly(2-oxazoline)s—Are They More Advantageous for Biomedical Applications than Other Polymers? *Macromol. Rapid Commun.* **2012**, *33*, 1648−1662.
(42) Rossegger, E.; Schenk, V.; Wiesbrock, F. Design Strategies for Functionalized Poly(2-oxazoline)s and Derived Materials. *Polymers* **2013**, *5*, 956−1011.
(43) Tauhardt, L.; Kempe, K.; Gottschaldt, M.; Schubert, U. S. Poly(2-oxazoline) Functionalized Surfaces: From Modification to Application. *Chem. Soc. Rev.* **2013**, *42*, 7998−8011.
(44) Weitman, S. D.; Lark, R. H.; Coney, L. R.; Fort, D. W.; Frasca, V.; Zurawski, V. R.; Kamen, B. A. Distribution of the Folate Receptor Gp38 in Normal and Malignant Cell Lines and Tissues. *Cancer Res.* **1992**, *52*, 3396−3401.
(45) Ross, J. F.; Chaudhuri, P. K.; Ratnam, M. Differential Regulation of Folate Receptor Isoforms in Normal and Malignant Tissues in Vivo and in Established Cell Lines: Physiological and Clinical Implications. *Cancer* **1994**, *73*, 2432−2443.
(46) Zauner, W.; Ogris, M.; Wagner, E. Polylysine-Based Transfection Systems Utilizing Receptor-Mediated Delivery. *Adv. Drug Delivery Rev.* **1998**, *30*, 97−113.
(47) Colombo, P. E.; Boustta, M.; Poujol, S.; Pinguet, F.; Rouanet, P.; Bressolle, F.; Vend, M. Biodistribution of Doxorubicin-Alkylated Poly(L-lysine citramide imide) Conjugates in an Experimental Model of Peritoneal Carcinomatosis after Intraperitoneal Administration. *Eur. J. Pharm. Sci.* **2007**, *31*, 43−52.
(48) Zhou, Z. X.; Shen, Y. Q.; Tang, J. B.; Fan, M. H.; Van Kirk, E. A.; Murdoch, W. J.; Radosz, M. Charge-Reversal Drug Conjugate for Targeted Cancer Cell Nuclear Drug Delivery. *Adv. Funct. Mater.* **2009**, *19*, 3580−3589.
(49) Al-Jamal, K. T.; Al-Jamal, W. T.; Wang, J. T. W.; Rubio, N.; Buddle, J.; Gathercole, D.; Zloh, M.; Kostarelos, K. Cationic Poly-L-lysine Dendrimer Complexes Doxorubicin and Delays Tumor Growth in Vitro and in Vivo. *ACS Nano* **2013**, *7*, 1905−1917.
(50) Kenausis, G. L.; Voros, J.; Elbert, D. L.; Huang, N. P.; Hofer, R.; Ruiz-Taylor, L.; Textor, M.; Hubbell, J. A.; Spencer, N. D. Poly(L-lysine)-*g*-poly(ethylene glycol) Layers on Metal Oxide Surfaces: Attachment Mechanism and Effects of Polymer Architecture on Resistance to Protein Adsorption. *J. Phys. Chem. B* **2000**, *104*, 3298−3309.
(51) Falconnet, D.; Csucs, G.; Grandin, H. M.; Textor, M. Surface Engineering Approaches to Micropattern Surfaces for Cell-Based Assays. *Biomaterials* **2006**, *27*, 3044−3063.
(52) Delgado, A. V.; Gonzalez-Caballero, F.; Hunter, R. J.; Koopal, L. K.; Lyklema, J. Measurement and Interpretation of Electrokinetic Phenomena. *J. Colloid Interface Sci.* **2007**, *309*, 194−224.
(53) Malmberg, C. G.; Maryott, A. A. Dielectric Constant of Water from 0° to 100° C. *J. Res. Natl. Bur. Stand.* **1956**, *56*, 1−8.
(54) Luo, K. Q.; Yu, V. C.; Pu, Y. M.; Chang, D. C. Application of the Fluorescence Resonance Energy Transfer Method for Studying the Dynamics of Caspase-3 Activation during UV-Induced Apoptosis in Living HeLa Cells. *Biochem. Biophys. Res. Commun.* **2001**, *283*, 1054−1060.

DOI: 10.1021/am508399w
ACS Appl. Mater. Interfaces 2015, 7, 2919−2930

(55) Pidhatika, B.; Chen, Y.; Coullerez, G.; Al-Bataineh, S.; Textor, M. Tof-SIMS Analysis of Poly(L-lysine)-*graft*-poly(2-methyl-2-oxazoline) Ultrathin Adlayers. *Anal. Bioanal. Chem.* **2014**, *406*, 1509−1517.
(56) Pasche, S.; De Paul, S. M.; Voros, J.; Spencer, N. D.; Textor, M. Poly(L-lysine)-graft-poly(ethylene glycol) Assembled Monolayers on Niobium Oxide Surfaces: A Quantitative Study of the Influence of Polymer Interfacial Architecture on Resistance to Protein Adsorption by ToF-SIMS and in Situ OWLS. *Langmuir* **2003**, *19*, 9216−9225.
(57) Wagner, M. S.; Pasche, S.; Castner, D. G.; Textor, M. Characterization of Poly(L-lysine)-*graft*-poly(ethylene glycol) Assembled Monolayers on Niobium Pentoxide Substrates Using Time-of-Flight Secondary Ion Mass Spectrometry and Multivariate Analysis. *Anal. Chem.* **2004**, *76*, 1483−1492.
(58) Wu, Z.; Li, X. X.; Hou, C. Y.; Qian, Y. Solubility of Folic Acid in Water at pH Values between 0 and 7 at Temperatures (298.15, 303.15, and 313.15) K. *J. Chem. Eng. Data* **2010**, *55*, 3958−3961.
(59) Wagner, M. S.; Castner, D. G. Characterization of Adsorbed Protein Films by Time-of-Flight Secondary Ion Mass Spectrometry with Principal Component Analysis. *Langmuir* **2001**, *17*, 4649−4660.
(60) Gabizon, A.; Horowitz, A. T.; Goren, D.; Tzemach, D.; Mandelbaum-Shavit, F.; Qazen, M. M.; Zalipsky, S. Targeting Folate Receptor with Folate Linked to Extremities of Poly(ethylene glycol)-Grafted Liposomes: In Vitro Studies. *Bioconjugate Chem.* **1999**, *10*, 289−298.
(61) Stella, B.; Arpicco, S.; Peracchia, M. T.; Desmaele, D.; Hoebeke, J.; Renoir, M.; D'Angelo, J.; Cattel, L.; Couvreur, P. Design of Folic Acid-Conjugated Nanoparticles for Drug Targeting. *J. Pharm. Sci.* **2000**, *89*, 1452−1464.
(62) Kim, Y. K.; Choi, J. Y.; Yoo, M. K.; Jiang, H. L.; Arote, R.; Je, Y. H.; Cho, M. H.; Cho, C. S. Receptor-Mediated Gene Delivery by Folate-PEG-Baculovirus in Vitro. *J. Biotechnol.* **2007**, *131*, 353−361.
(63) Liang, B.; He, M. L.; Xiao, Z. P.; Li, Y.; Chan, C. Y.; Kung, H. F.; Shuai, X. T.; Peng, Y. Synthesis and Characterization of Folate-PEG-Grafted-Hyperbranched-PEI for Tumor-Targeted Gene Delivery. *Biochem. Biophys. Res. Commun.* **2008**, *367*, 874−880.

DOI: 10.1021/am508399w
ACS Appl. Mater. Interfaces 2015, 7, 2919−2930